JOURNAL OF SOLID STATE CHEMISTRY 115, 112–119 (1995)

Crystal Structure and Conductivity of the New Superionic Conductor $Ag_4Hf_3S_8$

Olivier Amiel[1] and Hiroaki Wada

National Institute for Research in Inorganic Materials, 1-1 Namiki, Tsukuba-shi, Ibaraki 305, Japan

Received February 24, 1994; accepted June 15, 1994

$Ag_4Hf_3S_8$, prepared from a Ag_2S, Hf, and S mixture heated for 1 week at 650°C, crystallizes in the cubic system (space group $P4_332$) with lattice constant $a = 10.9051(2)$ Å ($Z = 4$, $\rho = 6.27$ g cm^{-3}). The crystal structure refinement from four-circle X-ray data yields a reliability factor R of 4.2%. The 32 S atoms, distributed over two different positions, 24*e* and 8*c*, produce 32 octahedra in the unit cell, each one being connected three-dimensionally with 12 other octahedra by sharing edges. The Hf atoms (12*d* sites)are located in sulfur octahedra. The Ag atoms are distributed over three different sites: Ag1 in the 8*c* positions and Ag2 and Ag3 in two general 24*e* positions, each of them being occupied statistically (occupancy = $\frac{1}{6}$). $Ag_4Hf_3S_8$ is a mixed conductor exhibiting a relatively high ionic conductivity. This compound becomes more conductive above 137°C due to the transition from a low-temperature ordered phase to a high-temperature disordered one (σ_{Ag^+} reaches 2.27×10^{-2} Ω^{-1} cm^{-1} at 198°C).

INTRODUCTION

Superionic conductive materials have been widely studied the past two decades for practical use as solid state electrolytes, for example (1). Due to their attractive ionic conduction properties, Ag-containing chalcogenides appear to be promising candidates. Many compounds of general chemical formula $Ag_\alpha M_\beta^{n+} X_\gamma$ (X = S, Se, Te) have been prepared and characterized from a crystallographic point of view (2). Especially, the compounds with $\alpha + n\beta = 2\gamma$, $\alpha \geq \beta$ and $\gamma = 2, 3, 6, 8$ are known to exhibit relatively higher Ag-ionic conductivity. However, ternary systems including M cations belonging to the IVb transition elements were almost not investigated except for titanium. Although most of the previously discovered compounds are structurally well characterized, little is known about the conduction mechanisms of silver ions in such structures. In order to attempt to make clear this phenomenon of fast ionic conduction, it appears essential to collect as much data as possible on Ag-containing multi-component systems. For these reasons, we studied the Ag–Hf–X systems, and during this work, the new compound $Ag_4Hf_3S_8$ was discovered. This paper describes the preparation, the crystallographic characterization, and the conduction properties of this new superionic conductive material.

[1] To whom correspondence should be addressed.

EXPERIMENTAL

Synthesis

The $Ag_4Hf_3S_8$ compound was synthesized from a stoichiometric mixture of Ag_2S (99.9%, Rare Metallic), Hf (99.9%, Rare Metallic), and S (99.9999%, Rare Metallic). The starting materials were mixed under an atmosphere of nitrogen inside a dry box, in order to avoid oxidation of the elements, and ground in an agate mortar. This mixture was pressed into pellets, introduced into a silica tube, and sealed at pressure of less than 10^{-3} Torr. The tube was then placed in a furnace and held at 650°C for 1 week. After preparation, samples were quenched in water. Single crystals were obtained by resuming the heating treatment at 1100°C for 2 weeks. Crystals of about 50 μm in size grew on the surface of the pellet by solid state reaction.

Analyses

X-ray powder diffraction intensity data were collected with a step-scan procedure using the graphite-monochromated Cu$K\alpha$ radiation of a Rigaku diffractometer (Geigerflex, RAD-2B system). In order to examine the crystal symmetry, single-crystals were characterized with a Buerger precession camera from Rigaku instruments (4012 K 2 type). The crystallographic study was performed on an Enraf-Nonius CAD-4 diffractometer, and the unit cell parameters were obtained by a least-squares analysis of the setting angles of 21 reflections automatically centered in the range of $27 \leq 2\theta(\text{Mo}K\alpha_1) \leq 32°$. Intensity data were collected by the ($\omega - \theta$) scan technique. A coefficient accounting for secondary isotropic extinction was refined and applied to the calculated struc-

0022-4596/95 $6.00

TABLE 1
Crystallographic Data and Conditions for Intensity Data Collection

Chemical formula	$Ag_4Hf_3S_8$
Formula weight (g)	1223
Space group	$P4_332$ (No. 212)
a (Å)	10.9051(2)
Volume (Å^3)	1296.85(3)
Z	4
Calculated density (g cm^{-3})	6.27
Measured density (g cm^{-3})	6.26
Temperature of data collection (°C)	23
Radiation monochromated λ (Mo$K\alpha$) (Å)	0.71073
Crystal shape	Spherical
Crystal color	Gray–black
Crystal size (mm)	Diameter = 0.04
Linear absorption coefficient μ (cm^{-1})	307.731
Transmission factors	0.187–0.219
Scan type	$\omega - \theta$
Scan speed	Variable
Scan range	(0.6 + 0.35 tan θ)
2θ (max)	70°
Data collected	$\pm h$, $+k$, $+l$ ($m3m$)
No. of reflections measured	1248
No. of unique reflections	979
No. of refined reflections with $I_o > 1.5\ \sigma\ I_o$	734
R_{int}	0.036
R (F)	0.042
R_w (F)	0.048

ture factors. Spherical absorption and Lorentz-polarization corrections were also applied to the data. Some additional conditions for data collection are summarized in Table 1. Density measurements were carried out by the immersion method described by Barker, in which CCl_4 was used as solvent (3).

Both the ionic conductivity of silver and the total conductivity of $Ag_4Hf_3S_8$ were measured by a dc method using a Solartron 1286 electrical interface. The measurements were made on polycrystalline samples pressed (applied pressure = 7 tonnes) into pellet (diameter = 7.7 mm). The experimental cell was introduced into a glass tube under argon atmosphere, to avoid oxidation of the sample during experiments at higher temperature. Experiments were performed using a constant current (less than 10^{-3} A) and measuring the resulting voltage drop across the sample. Preliminary experiments confirmed that interfacial polarization of the interfaces was negligible under these experimental conditions.

RESULTS AND DISCUSSION

Structure Determination

Before four-circle X-ray experiments, the X-ray powder diffraction pattern of $Ag_4Hf_3S_8$ was firstly refined in the cubic system giving a lattice parameter a = 10.9015(4) Å and a cell volume V = 1295.5(1) Å^3 (Fig. 1). Then, crystal symmetry and suitability for intensity data collection were checked by the means of the Buerger precession camera. Photographs indicated that $Ag_4Hf_3S_8$ crystallizes in space group $P4_332$ or $P4_132$, both characterized by the same systematic reflection condition:

$$0\ 0\ l;\ l = 4n.$$

On the basis of previous work (4), the structure was solved, using data obtained from four-circle experiments, by the direct method (MULTAN method) in space group $P4_332$ (No. 225) and refined on F^2 by the full-matrix least-squares method (5). The conventional $R(F)$ factor for reflections corresponding to $I_o > 1.5\ \sigma\ I_o$ is 0.042. Some crystallographic data are given in Table 1. The final positions and the equivalent isotropic and anisotropic thermal parameters are gathered in Table 2.

Structure Description

$Ag_4Hf_3S_8$ has a three-dimensional and close-packed structure. For clarity, the type of site and environment of each kind of atom will be discussed separately.

The 32 sulfur atoms distributed over two different fully occupied positions, 24e and 8c, produce 32 octahedra in the unit cell (Fig. 2). Each octahedron is connected three-dimensionally with 12 other octahedra by sharing the edges.

The hafnium atoms are distributed over 12d positions only, and are located in octahedra constituted of sulfur atoms. The projection in the (a, b) plane corresponds to a cross section of the structure following the c-axis for a value of z equal to 0.6352 (Fig. 3). Within the same HfS_6 sheet, octahedra are linked together by edges and the sequence (3 octahedra—vacancy—3 octahedra) is observed. Figure 4a presents the superposition of the previous cross section at z = 0.6352 together with the lower one at z = 0.3852; Fig. 4b corresponds to the superposition of the previous cross section at z = 0.6352 together with the upper one at z = 0.8852. These two figures elucidate the three-dimensional packing of the HfS_6 octahedra. From one HfS_6 sheet to the other one (along the c-axis), octahedra are sharing edges and the packing alternates between the [1 1 0] direction and the [$\bar{1}$ 1 0] direction. In each elementary octahedron, the hafnium atom is surrounded by four sulfur S1 and two sulfur S2. Considering the projection in the (a, b) plane, sulfur atoms in equatorial positions are S1(5), S1(6), S1(1), and S2(3), and the bond lengths with hafnium atoms range from 2.495(2) to 2.577(2) Å, as shown in Table 3. Sulfur atoms in axial positions are S1(4) (up) and S2(5) (down), and the corresponding Hf–S distances are 2.495(2) and 2.577(2)Å, respectively.

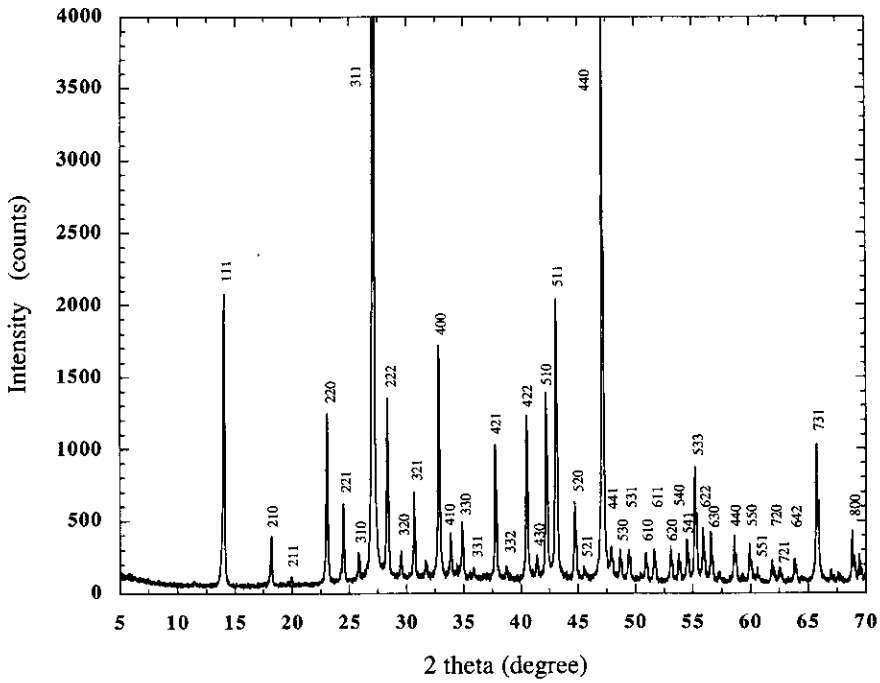

FIG. 1. X-ray powder diffraction pattern of $Ag_4Hf_3S_8$.

Silver atoms Ag1 are distributed over 8*c* positions and are located in nearly regular sulfur tetrahedra. Figure 5 represents Ag1 atoms and some corresponding tetrahedra. In each AgS_4 elementary tetrahedron, the silver atom Ag1 is surrounded by three sulfur S1 and one sulfur S2. Bond lengths and angles within this type of tetrahedron are gathered in Table 4. The distances between Ag1 and S1 are all equal to 2.548(3) Å whereas that between Ag1 and S2 is a bit longer and equal to 2.572(1) Å.

Silver atoms Ag2 and Ag3 are distributed over two statistically occupied general positions, 24*e*. Tables 5 and 6 give the main interatomic distances and angles for Ag2 and Ag3 polyhedra, respectively. Figure 6 corresponds to the projection in the (*a*, *b*) plane of Ag1, Ag2, and Ag3

TABLE 2
Atomic Coordinates, Site Type and Occupancy, Equivalent Isotropic and Anisotropic Thermal Factors for $Ag_4Hf_3S_8$

	Atom					
	Hf	Ag_1	Ag_2	Ag_3	S_1	S_2
Wyckoff notation	12*d*	8*c*	24*e*	24*e*	24*e*	8*c*
x	0.625	0.0073(1)	0.313(1)	0.2143(8)	0.3924(2)	0.8711(2)
y	0.1148(1)	0.0073(1)	0.179(1)	−0.0195(9)	0.0927(2)	0.8711(2)
z	0.1351(1)	0.0073(1)	0.968(1)	0.330(1)	0.1442(3)	0.8711(2)
Site occupancy	1	1	0.1667	0.1667	1	1
B(1, 1)	1.12(1)	2.24(2)	8.3(6)	5.6(3)	0.93(7)	0.87(4)
B(2, 2)	1.016(8)	2.24(2)	10.0(8)	5.4(3)	0.90(7)	0.87(4)
B(3, 3)	1.016(8)	2.24(2)	4.7(4)	8.8(6)	3.0(1)	0.87(4)
B(1, 2)	−0.04(1)	−0.20(3)	3.2(4)	4.5(2)	0.08(6)	0.11(6)
B(1, 3)	−0.04(1)	−0.20(3)	−3.7(3)	3.8(3)	−0.00(8)	0.11(6)
B(2, 3)	−0.07(1)	−0.20(3)	2.1(3)	2.2(4)	−0.26(7)	0.11(6)
B(eq)[a]	1.050(5)	2.238(7)	7.7(3)	6.6(2)	1.61(4)	0.87(1)

[a] $B(\text{eq}) = (8\pi^2/3) \sum_i \sum_j U_{ij} a_i^* a_j^* a_i a_j = 4/3 \sum_i \sum_j B_{ij} a_i a_j$.

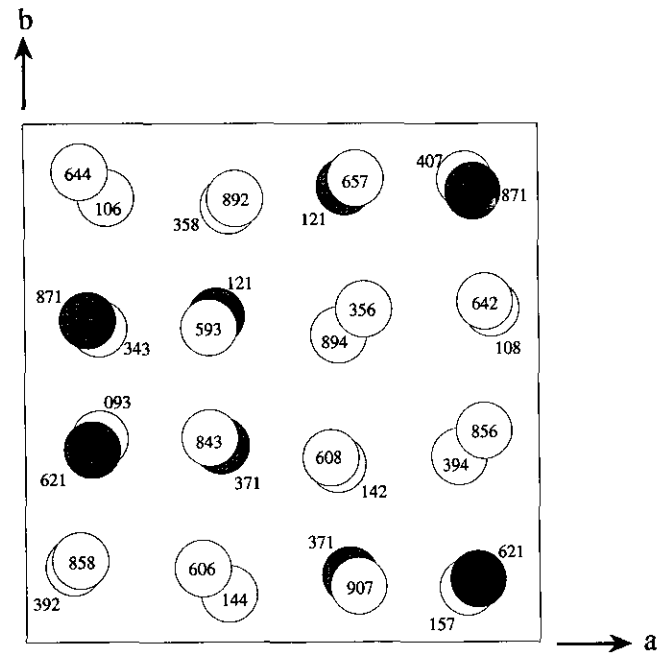

FIG. 2. Projection in the (a, b) plane of S1 and S2 sulfur atoms. Numbers indicate the z parameter values of the corresponding atoms, in 1/1000s. White and shaded atoms correspond to S1 and S2, respectively.

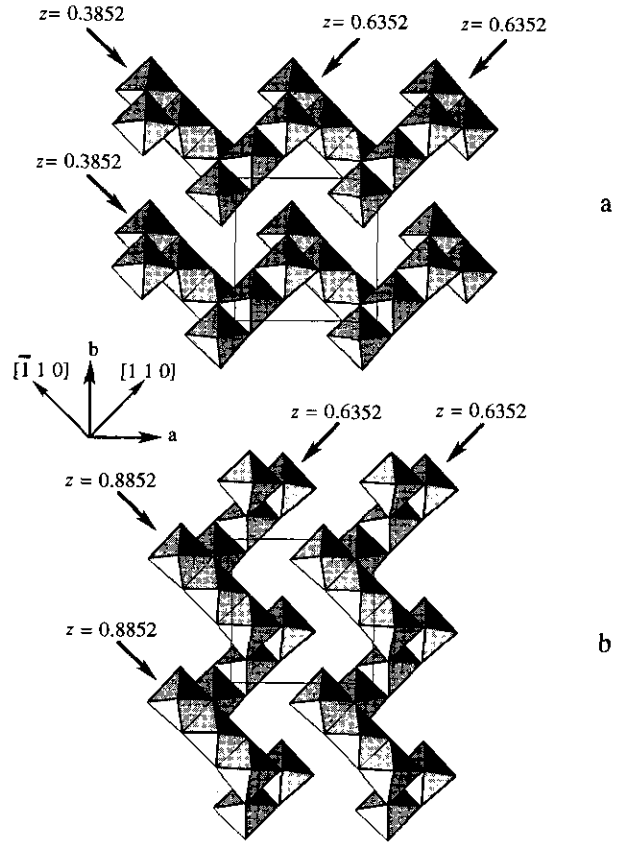

FIG. 4. Projection in the (a, b) plane of (a) the superposition of the cross sections at z = 0.6352 and z = 0.3852; (b) the superposition of the cross sections at z = 0.6352 and z = 0.8852.

silver atoms. These atoms form into a shape resembling a bow tie made up of two rings, each of them consisting of six Ag2 and six Ag3 possible positions. The very close positions of Ag2 and Ag3 lead, from a crystallographic point of view, to unacceptable Ag2–Ag3 distances of 0.45(2) Å, much shorter than twice the ionic radius of a silver ion. Short Ag–Ag distances were commonly observed in the case of superionic conductive chalcogenides (6–11). In fact, the occupancy of these two kinds of site is $\frac{1}{6}$; therefore only one Ag2 and one Ag3 positions are occupied at each instant. This structural feature illustrates the mobile character of silver ions which can migrate in a liquid-like manner by jumping between vacant sites at higher temperatures. The tendency of silver ions to form aggregates is noteworthy and seems independent of the nature of the anion as Jansen observed the same behavior in the case of silver ternary oxide (12). The electronic structure of the silver ions, namely d^{10}, appears to be the main factor as similar results were obtained with copper (d^{10})-containing ternary systems. Figure 7 shows the structure of an elementary ring. For clarity, only Ag2 positions are represented but identical results are obtained in the case of Ag3 positions. The Ag2(2), Ag2(4), and Ag2(6) positions form an equilateral triangle, each side corresponding to an Ag2–Ag2 distance equal to 2.33(2) Å. The Ag2(1), Ag2(3), and Ag2(5) positions also form an equilateral triangle of same Ag2–Ag2 distance, but located on an upper plane. Bond lengths between Ag2 atoms, from one plane to the other, are successively 1.47(2) Å and 1.28(2) Å (Fig. 7). The small Ag–Ag distances between adjacent sites prevent these from being simultaneously occupied. Two different coordination geometries may be used to characterize the environment of an Ag2 (or Ag3) atom: (i) the Ag2 site may be described as a tetrahedron

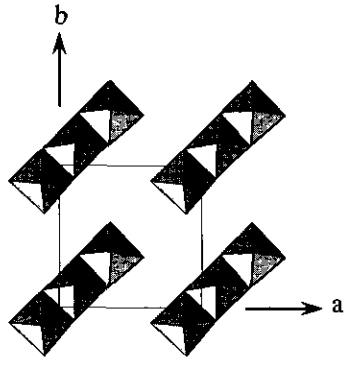

FIG. 3. Projection in the (a, b) plane of the cross section of the structure for z = 0.6352.

TABLE 3
Selected Bond Lengths and Angles Describing the Environment of Hf Atoms

Interatomic distances	(Å)
Hf–S1(1)	2.495(2)
Hf–S1(4)	2.495(2)
Hf–S1(5)	2.550(2)
Hf–S1(6)	2.550(2)
Hf–S2(2)	2.577(2)
Hf–S2(3)	2.577(2)
Angles	(°)
S1(6)–Hf–S1(4)	90.53(9)
S1(6)–Hf–S1(5)	169.19(2)
S1(6)–Hf–S2(3)	89.06(8)
S1(6)–Hf–S2(2)	83.77(7)
S1(6)–Hf–S1(1)	96.9(1)
S1(4)–Hf–S1(5)	96.9(1)
S1(4)–Hf–S2(3)	84.87(6)
S1(4)–Hf–S2(2)	174.01(8)
S1(4)–Hf–S1(1)	94.00(8)
S1(5)–Hf–S2(3)	83.77(7)
S1(5)–Hf–S2(2)	89.06(8)
S1(5)–Hf–S1(1)	90.53(9)
S1(3)–Hf–S2(2)	96.9(1)
S1(3)–Hf–S1(1)	174.01(8)
S1(2)–Hf–S1(1)	84.87(6)

TABLE 4
Selected Bond Lengths and Angles Describing the Environment of Ag1 Atoms

Interatomic distances	(Å)
Ag1–S1(1)	2.548(3)
Ag1–S1(2)	2.548(3)
Ag1–S1(3)	2.548(3)
Ag1–S2(4)	2.572(1)
S1(1)–S1(2)	4.280(4)
S1(1)–S1(3)	4.280(4)
S1(1)–S2(4)	4.039(3)
S1(2)–S1(3)	4.280(4)
S1(2)–S2(4)	4.039(3)
S1(3)–S2(4)	4.039(3)
Angles	(°)
S1(1)–Ag1–S1(2)	114.24(9)
S1(1)–Ag1–S1(3)	114.24(9)
S1(1)–Ag1–S2(4)	104.13(6)
S1(2)–Ag1–S1(3)	114.24(9)
S1(2)–Ag1–S2(4)	104.13(6)
S1(3)–Ag1–S2(4)	104.13(6)

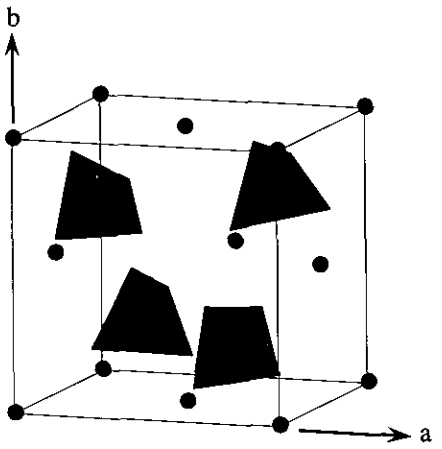

FIG. 5. View of Ag1 atoms (black circles) and corresponding tetrahedra in the unit cell.

site made up of S1-type sulfur atoms exclusively, but in that case the bond Ag2(1)–S1(2), equal to 3.26(1) Å, is very long compared to the others; (ii) the Ag2 site may be described as a triangular site in which the silver atom is located slightly outside of the face made up of S1(1), S1(3), and S1(4) atoms (distance from the surface of the face was calculated to be 0.228(1) Å). Each Ag2 (or Ag3) tetrahedron is connected with an Ag1 tetrahedron by a 4.280(1) Å long edge made up of S1(2) and S1(3) atoms (Fig. 7).

Conductivity Properties of $Ag_4Hf_3S_8$

A schematic diagram of the measurement cell is represented in Fig. 8. For ionic conductivity measurement, the

TABLE 5
Selected Bond Lengths and Angles Describing the Environment of Ag2 Atoms

Interatomic distances	(Å)
Ag2–S1(1)	2.75(1)
Ag2–S1(2)	3.26(1)
Ag2–S1(3)	2.31(1)
Ag2–S1(4)	2.57(1)
S1(1)–S1(2)	3.584(4)
S1(1)–S1(3)	4.666(4)
S1(1)–S1(4)	3.774(4)
S1(2)–S1(3)	4.280(4)
S1(2)–S1(4)	3.650(4)
S1(3)–S1(4)	4.476(4)
Angles	(°)
S1(1)–Ag2–S1(2)	72.6(3)
S1(1)–Ag2–S1(3)	134.0(5)
S1(1)–Ag2–S1(4)	90.2(4)
S1(3)–Ag2–S1(2)	98.9(4)
S1(3)–Ag2–S1(4)	132.7(5)
S1(2)–Ag2–S1(4)	76.4(3)

TABLE 6
Selected Bond Lengths and Angles Describing the Environment of Ag3 Atoms

Interatomic distances	(Å)
Ag3–S1(1)	2.86(1)
Ag3–S1(2)	3.06(1)
Ag3–S1(3)	2.32(1)
Ag3–S1(4)	2.49(1)
S1(1)–S1(2)	4.280(4)
S1(1)–S1(3)	4.476(4)
S1(1)–S1(4)	4.666(4)
S1(2)–S1(3)	3.650(4)
S1(2)–S1(4)	3.584(4)
S1(3)–S1(4)	3.774(4)
Angles	(°)
S1(1)–Ag3–S1(2)	76.0(3)
S1(1)–Ag3–S1(3)	119.0(4)
S1(1)–Ag3–S1(4)	89.5(3)
S1(3)–Ag3–S1(2)	104.3(4)
S1(3)–Ag3–S1(4)	151.5(5)
S1(2)–Ag3–S1(4)	79.7(3)

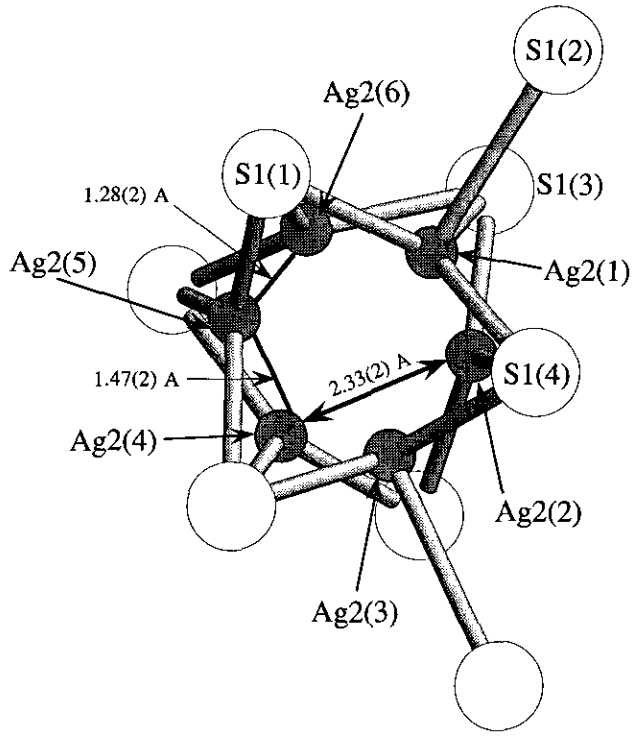

FIG. 7. Structure of an elementary ring consisting of Ag2 atoms.

arrangement Ag/$RbAg_4I_5$/sample/$RbAg_4I_5$/Ag was used, in which $RbAg_4I_5$ acts as an electron blocking layer. In the case of total conductivity measurement, the setup was simply Ag/sample/Ag. Experimental results obtained both from ionic and total conductivity measurements are plotted in Fig. 9. The log σ_{Ag+} for $Ag_4Hf_3S_8$ is -4.47 at 27°C and increases linearly to -3.59 at 137°C with an activation energy of 0.22 eV. The compound becomes subsequently more conductive reaching a value of log σ_{Ag+} equal to -1.83 at 180°C, with an activation energy of 1.52 eV. This change in conductivity is probably due to some transition from a low-temperature ordered phase to a high-temperature more disordered one. From 180 to 200°C, the ionic conductivity log σ_{Ag+} slightly increases to -1.65 with an activation energy of 0.44 eV. The similar behavior of ionic and total conductivity curves would suggest that electronic conductivity is almost independent of the temperature. The transport number of Ag^+, expressed as $\sigma_{Ag+}/(\sigma_{Ag+} + \sigma_{e-})$, was evaluated to be 0.23 between 28 and 105°C, meaning that $Ag_4Hf_3S_8$ is a mixed conductor.

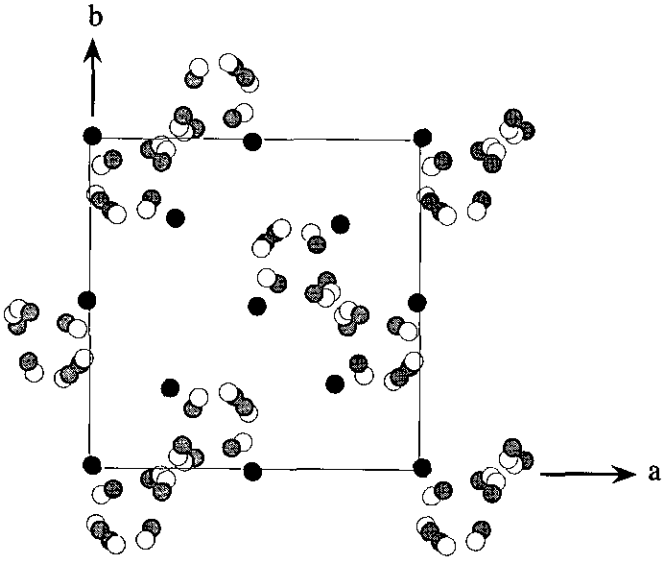

FIG. 6. Projection in the (a, b) plane of Ag1 (black circles), Ag2 (shaded circles), and Ag3 (white circles) atoms.

Correlations between Crystallographic Structure and Ionic Conductivity Properties

The theoretical description of the transport of silver ions is a very complex problem because the occupancies

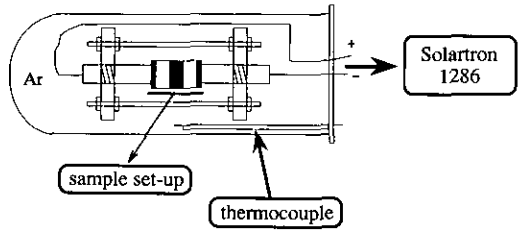

FIG. 8. Schematic diagram of the experimental apparatus used to measure ionic and total conductivities.

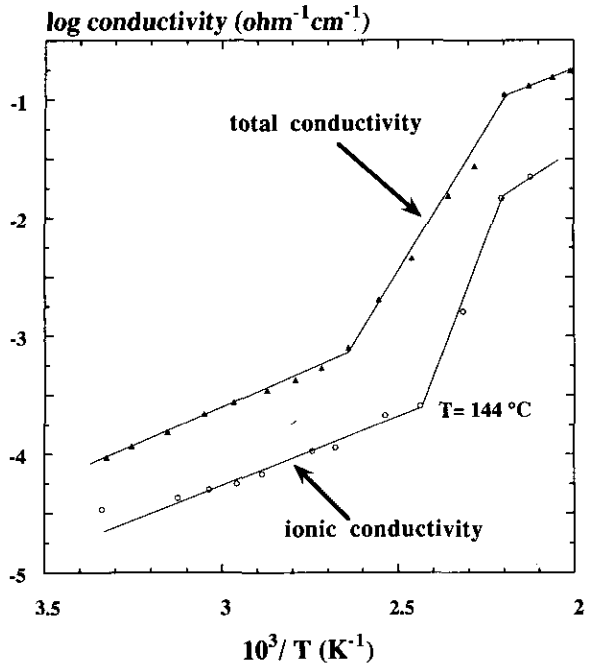

FIG. 9. Ag^+ ionic conductivity and total conductivity of $Ag_4Hf_3S_8$ versus temperature.

of the sites available for silver ions are very low and result in a disordered arrangement of silver ions. Moreover, the frequency of cation jumps to neighboring sites is not constant and depends on the distribution of cations in the vicinity of the cation considered (13). Numerous investigations have been made to clarify the ionic conductivity of such materials. Even if a single and unique model cannot explain the ionic transport of all the superionic conductive materials, some general rules may be stated from previous studies:

(i) The lower the coordination of the mobile ion, the lower the activation energy is, as the Coulomb forces are less important. Tetrahedral sites sharing faces seem to be the ideal configuration for the best conduction (14, 15).

(ii) The ionic transport is controlled by the potential barriers in between the sites, but the importance of motion between the sites is also emphasized by the density distribution of mobile ions (16).

(iii) The arrangement of polyhedra between each other also plays a great role. The network of silver ions conducting passageways is formed by the face sharing of sulfur ion polyhedra allowing direct passages from one site to the other (17). Depending on the crystallographic structure, there is a large variety of possible passageways through the anion lattice.

(iv) For a given network of possible passageways, different transport mechanisms may be considered. In his paper, Geisel proposes a complete survey of the possible transport mechanisms of a small particle moving in a host lattice (16). Among them, the "caterpillar" mechanism, which is the most commonly used, assumes that an ion on a site is able to jump not only into a vacant neighboring site but also into an occupied one, inducing the ion on the latter site to jump in the same direction or at least, in a positively correlated direction. This process continues until one of the cations finds a vacancy to fill. But this kind of cooperative mechanism alone is not sufficient and satisfactory to explain ionic conductivity. In fact, a superposition of jump-diffusion and a local kind of motion characterized by large amplitudes and strong damping seems to better describe the conduction mechanism (18).

Although the exact description of the passageways involved in the conduction mechanism is a complex problem, it may be interesting to attempt to establish some correlations between the structure of $Ag_4Hf_3S_8$ and the

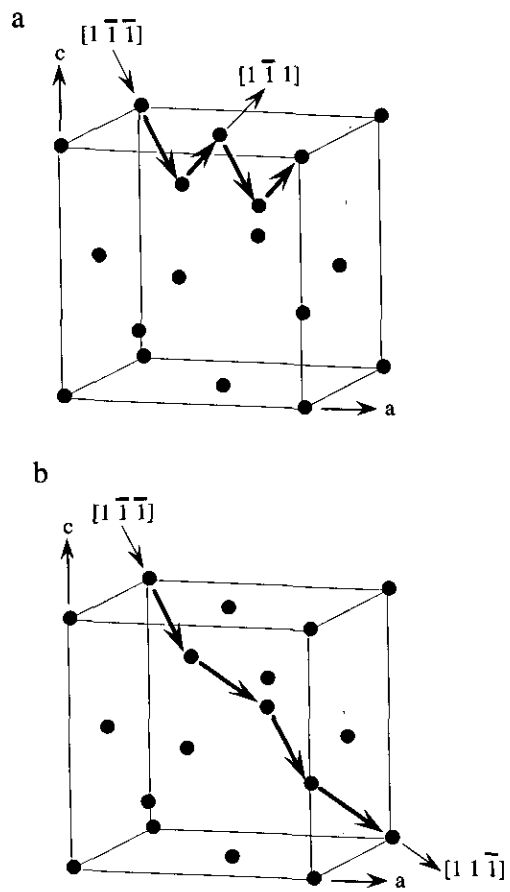

FIG. 10. Schematic representation of two possible passageways for AgI ions, corresponding to zigzag caterpillar mechanisms (a) alternatively in the [1 $\bar{1}$ $\bar{1}$] and [1 $\bar{1}$ 1] directions (b) alternatively in the [1 $\bar{1}$ $\bar{1}$] and [1 1 $\bar{1}$] directions.

ionic conductivity behavior. According to the low occupancies of Ag2 and Ag3 sites, the low coordination of silver atom (3 or 4) and the very short Ag2–Ag2, Ag3–Ag3, and Ag2–Ag3 distances, it may be reasonable to explain the first part of the ionic conductivity curve ($26 \leq T \leq 137$°C, $E_a = 0.22$ eV) by motions involving jumps between Ag2 and Ag3 positions. As the temperature is increased, silver ions move from (Ag2, Ag3) sites to Ag1 sites, the distance between the two sites being 3.159(1)Å. As Ag2 (or Ag3) and Ag1 tetrahedra are sharing edges (and not faces), the potential barriers corresponding to passageways between these two kinds of tetrahedra is higher in energy, as shown by the strong value of the activation energy ($E_a = 1.52$ eV) between 137 and 180°C. Above this temperature, jumps between Ag1 tetrahedra may occur. Different passageways have to be considered. The first one corresponds to a zigzag caterpillar transport mechanism alternatively in the [1 $\bar{1}$ $\bar{1}$] and [1 $\bar{1}$ 1] directions. In such a mechanism, jump lengths between Ag1 ions range from 4.444(1) to 4.816(1) Å (Fig. 10a). The second one also corresponds to a zigzag caterpillar transport mechanism, but alternatively in the [1 $\bar{1}$ $\bar{1}$] and [1 1 $\bar{1}$] directions, and jump lengths are in the same range (Fig. 10b). These passageways are characterized by low activation energy ($E_a = 0.44$ eV for $180 \leq T \leq 200$°C) and are the most probable as they involve the shortest Ag–Ag distances.

The aim of this last section is not to give the exact description of the ionic conductivity occurring in $Ag_4Hf_3S_8$ but to propose some possible passageways for silver ions, with regard to the structural features of this compound.

REFERENCES

1. B. B. Owens and P. M. Skarstad, *in* "Fast Ion Transport in Solids" (Vashishta, Mundy, and Shenoy, Eds.), pp. 61–67. Elsevier–North Holland, Amsterdam, 1979.
2. B. Eisenmann and H. Schafer, *in* "Landolt–Bornstein: Numerical Data and Functional Relationships in Science and Technology—New Series" (K.-H. Hellewege and A. M. Hellewege, Eds.), Group III, Vol. 14, Subvol. b. Springer-Verlag Berlin/Heidelberg/New York/Tokyo, 1986.
3. W. W. Barker, *J. Appl. Crystallogr.* **5,** 433 (1972).
4. A. W. Henfrey and B. E. F. Fender, *Acta Crystallogr. B* **26,** 1882 (1970).
5. B. A. Frenz & Associates, Inc. "SDP Structure Determination Package," 4th ed. College Station, Texas, 1985.
6. H. Wada and M. Onoda, *J. Less-Common Met.* **175,** 209 (1991).
7. H. Wada, *J. Alloys Comp.* **178,** 315 (1992).
8. N. Rysanek, P. Laruelle, and A. Katty, *Acta Crystallogr. B* **32,** 692 (1976).
9. J. P. Deloume, R. Faure, H. Loiseleur, and M. Roubin, *Acta Crystallogr. B.* **34,** 3189 (1978).
10. S. Geller, *Z. Kristallogr.* **149,** 31 (1979).
11. J. P. Deloume and R. Faure, *J. Solid State Chem.* **36,** 112 (1981).
12. M. Jansen, *Angew. Chem. Int. Ed. Engl.* **26,** 1098 (1987).
13. D. Grientschnig and W. Sitte, *J. Phys. Chem. Solids* **52**(6), 805 (1991).
14. B. Cros, A. Zerouale, M. Pintard, E. Philippot, and M. Ribes, *Eur. J. Solid State Inorg. Chem.* **25,** 541 (1988).
15. P. Vashishta and A. Rahman, *in* "Fast Ion Transport in Solids" (Vashishta, Mundy, and Shenoy, Eds.), pp. 527–533. Elsevier–North Holland, Amsterdam, 1979.
16. T. Geisel, *in* "Fast Ion Transport in Solids" (Vashishta, Mundy, and Shenoy, Eds.), pp. 541–546, Elsevier–North Holland, Amsterdam, 1979.
17. T. Takahashi, *in* "Fast Ion Transport in solids" (Vashishta, Mundy, and Shenoy, Eds.), pp. 521–526. Elsevier–North Holland, Amsterdam, 1979.
18. K. Funke, *Prog. Solid State Chem.* **11,** 345 (1976).